Pergamon

Bioorganic & Medicinal Chemistry 10 (2002) 4131–4141

BIOORGANIC & MEDICINAL CHEMISTRY

Characterization of a Binding Site for Template Competitive Inhibitors of HIV-1 Reverse Transcriptase Using Photolabeling Derivatives†

Weiying Lin,[a] Ke Li[a] and Michael B. Doughty[a,b,*]

[a]*Department of Medicinal Chemistry, The University of Kansas, Lawrence, KS 66045, USA*
[b]*Department of Chemistry and Physics, Southeastern Louisiana University, Hammond, LA, USA*

Received 4 March 2002; accepted 31 May 2002

Abstract—Analogues of a novel class of template-competitive reverse transcriptase inhibitors (Li, K.; Lin, W.; Chong, K. H.; Moore, B. M.; Doughty, M. B. *Bioorg. Med. Chem.* **2002**, *10*, 507) were analyzed as photoprobes of HIV-1 reverse transcriptase (RT) heterodimer. The two photoprobes, 2-(4-azidophenacyl)thio-1,N^6-etheno-2′-deoxyadenosine 5′-triphosphate **2** and the tetrafluoro analogue 2-(4-azido-2,3,5,6-tetrafluorophenacyl)thio-1,N^6-etheno-2′-deoxyadenosine 5′-triphosphate **3**, photodecomposed at 3500 Å with half-lives of 4.0 and 2.5 min, respectively. Analysis of the photoproducts of **2m** demonstrated that the etheno group is stable but the azido decomposes primarily to the 2-(*S*-[3H-diazepinon-4-yl]thio)-1,N^6-etheno-dAMP. Photolysis of both **2** and **3** with RT resulted in a time-dependent loss of activity, with maximum inactivation of 83 and 60%, respectively. Both **2** and **3** showed concentration-dependent photoinactivation of RT in the concentration range from 0 to 100 μM, with EC_{50}s of 20 and 25 μM and maximum inactivation of 80 and 60%, respectively. Both the time and concentration dependent photoinactivation were strongly protected by template-primer, but only poorly inhibited by even high concentrations of TTP. Radiolabeled analogues [β,γ-^{32}P]-2 and [β,γ-^{32}P]-**3** photoincorporated into the p66 subunit, an incorporation also protected by template primer. Identification of the site of incorporation was problematic for both photoprobes, but evidence presented is consistent with labeling sites for the phenacyl side chains of both **2** and **3** in the template grip. Nevertheless, the photoinactivation and incorporation data are consistent with our earlier conclusions from the kinetic data that these inhibitors are specific for the free form of RT in competition with template/primer, and thus represent a novel class of inhibitors.

Introduction

HIV-1 reverse transcriptase (RT) is a multifunctional enzyme that plays essential roles in HIV-1 replication, and the enzyme has therefore been an important target for drug therapy. The major functions of RT include RNA-dependent DNA polymerase, DNA-dependent DNA polymerase, and ribonuclease H activities, and the active sites for these activities reside on the p66 subunit of the p51-p66 heterodimer.[1–3] The polymerase activities of RT catalyze the elongation of DNA in the 5′ to 3′ direction using RNA or DNA as a template.[1–6] Therapeutically significant classes of HIV-1 RT inhibitors include both nucleoside (NRTIs) and non-nucleoside (NNRTIs) analogues. NRTIs are activated in vivo to the corresponding triphosphates by cellular kinases, and are alternate substrates, binding competitively relative to dNTPs and uncompetitive to the template. The binding site(s) of the triphosphate-activated NRTIs is thought to be identical to that of dNTPs observed in the ternary complex crystal structure.[6] In contrast, NNRTIs are non-competitive to both the template/primer and dNTP, and photolabeling and crystallography evidence show that the NNRTIs bind to a region outside the substrate active sites.[3,7–12]

We recently reported a novel class of HIV-1 RT combined substrate inhibitors that we called the template-competitive RT inhibitors, or TCRTIs, based on kinetic characteristics.[13] The most active analogue in this series is the 2-benzylacylthio-1,N^6-etheno-2′-deoxyadenosine 5′-triphosphate **1**, with a competitive K_i of 6 μM, and

*Corresponding author. Tel.: +1-985-549-5123; fax: +1-985-549-5126; e-mail: mdoughty@selu.edu
†Taken in part from the dissertation of Dr. Weiying Lin, The University of Kansas, 2000 and in part from the dissertation of Dr. Ke Li, The University of Kansas, 1996.

0968-0896/02/$ - see front matter © 2002 Elsevier Science Ltd. All rights reserved.
PII: S0968-0896(02)00259-6

the phenacyl photoaffinity analogues **2** and **3** which have competitive K_i's of about 10 μM. This class of inhibitors is competitive with respect to template/primer binding, and non-competitive relative to dNTP substrate binding, indicating that they compete with template/primer for free RT and do not bind to the binary RT-template/primer complex as a dNTP substrate. Preliminary SAR studies demonstrated that the 2-position side chain (the 3-phenyl-2-propanone for **1** and the phenacyl for **2** and **3**), the 1,N^6-etheno group, and the triphosphate were all necessary modifications for RT inhibition (the analogue lacking the 1,N^6-etheno group is an inhibitor of DNA polymerase I Klenow fragment but is inactive as an RT inhibitor up to 1.0 mM[14,15]). Whether this class of inhibitors can represent a novel approach, or at least represent a novel target for further design, depends on knowledge of their binding site and preferred modifications. For this reason, we synthesized photoprobes **2** and **3** as representative structural probes of this class of RT inhibitors. In the current communication, we provide further data that supports our main conclusion that the TCRTIs as a class bind to free RT utilizing binding interactions at both the dNTP and template binding sites.

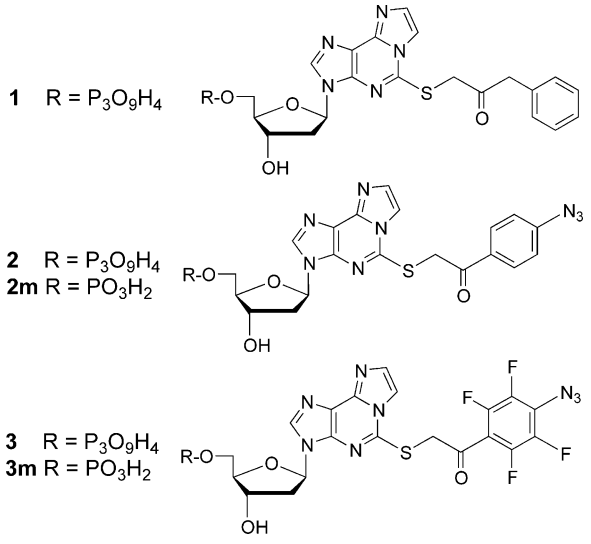

Results

Photochemistry of 2m and 3m

Photodecomposition of **2m** and **3m** (Fig. 1) was examined by monitoring the UV absorbance change upon irradiation at 3000 or 3500 Å in water-jacketed quartz cells. As shown in Figure 1, compounds **2m** and **3m** have absorption maxima at 297 and 315 nm, respectively. Overlays of the UV spectra taken at different times of irradiation show isobestic points at 244, 260 and 332 nm for **2m** and 267, 284 and 345 nm for **3m**, indicating single reaction pathways for the photodecomposition. Note that although the wavelength maxima for **3m** is shifted to the right by 24 nm (as expected for the electronic effect of the electron withdrawing fluorine groups), the spectra for the two compounds, including the positions of the isobestic points, have similar shapes. Photodecomposition followed first-order kinetics, with

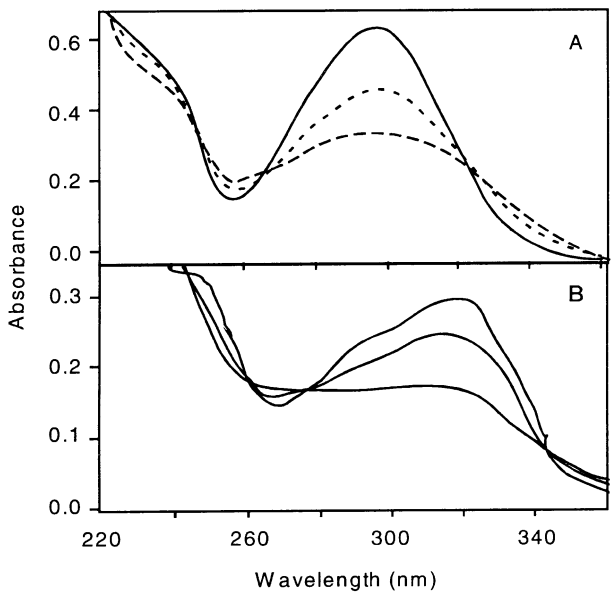

Figure 1. Photodecomposition of 2-(4-azidophenacyl)thio-1,N^6-etheno-dAMP **2m** (A) and the 2,3,5,6-tetrafluoro analogue **3m** (b). The spectra for A were taken at time 0 (top line), and at times 4 and 8 min after photolysis at 3500 Å. The spectra for B were taken at time 0 (top line), and at times 2 and 8 min after photolysis at 3500 Å. The photolysis mixtures were diluted 1/100 in phosphate buffer, pH 7.0 after photolysis. The spectra obtained were independent of the wavelength of photolysis with the exception that at 3000 Å photolysis the decomposition rate increased (see text for half-lives).

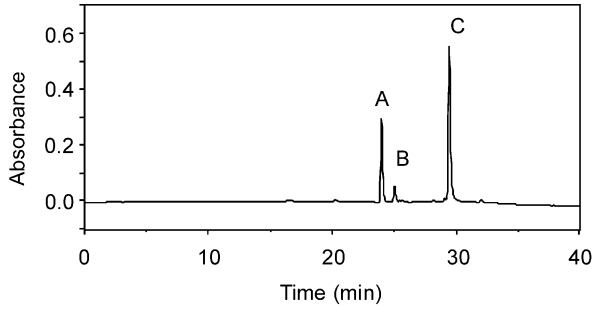

Figure 2. HPLC analysis of photolysis products of 2-(4-azidophenacyl)thio-1,N^6-etheno-dAMP (**2m**). Photoprobe **2m** was photolyzed for 1 min (at 1 mM concentration) in a quartz cuvette at 27 °C. The reaction mixture was then chromatographed on C18 reverse-phase eluting with 0–50% acetonitrile in neutral, 10 mM ammonium acetate.

half-lives for 0.6 and 4 min for **2m** and 0.5 and 2.5 min for **3m** at 3000 and 3500 Å, respectively.

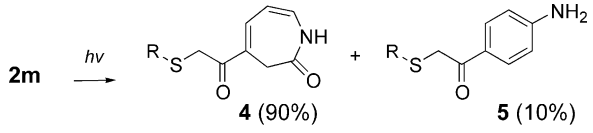

R = 1,N^6-etheno-2'-deoxyadenosin-2-yl 5'-monophosphate

In order to ensure that the photodecomposition involved only the azido and not the etheno group, photoprobe **2m** was analyzed for photoproducts after 50% photolysis (based on change in peak area versus time) at 3000 Å. An HPLC analysis of the reaction mixture (Fig. 2) displayed major and minor products eluting at 23.9 and 25.1 min, respectively; the third peak

eluting at 29.1 min (peak C) was identified as unreacted starting material. Isolation of each peak and analytical analysis by NMR and mass spectrometry indicate that the major peak results from rearrangement of the singlet nitrene and water capture to the 4-substituted azepinone **4**. The minor product is the amine **5**. In both photoproducts the etheno group is intact, demonstrating that the photodecomposition pathway observed is due to azide and not etheno decomposition. Additionally, the fact that the azepinone formed from the singlet nitrene is the predominant photolysis product of **2** is consistent with previous reports that aryl nitrenes with an acyl group substituted at *otho*- or *para*-positions react with weak nucleophiles, such as alcohols, to form alkoxyazepines.[16–18] It also suggests that covalent labeling of the enzyme by photoprobe **2m** can occur by reaction of a singlet carbene via a dehydroazepine intermediate with weak nucleophiles rather than through direct insertion. The tetrafluoro substituents in **3m** are known to stabilize the singlet nitrene against rearrangement chemistry leading to electrophiles, such that photolabeling can occur exclusively through singlet nitrene chemistry;[19,20] in this regard the triphosphate **3** gave a single photolysis product which eluted from HPLC reverse phase 5.3 min before the azide (data not shown) in a triethylammonium bicarbonate elution buffer.

Photoinactivation of HIV-1 RT by 2 and 3

In order to evaluate the photoinactivation of RT by photoprobes **2** and **3**, mixtures containing RT (2 μM) and various concentrations of the photoprobe were assembled and irradiated for up to 12 min at 3500 Å (RT rapidly degrades at 3000 Å photolysis, so only long wavelength photolysis was used in this study). The residual RT activity at each time point was determined after 100-fold dilution to afford a final concentration of the photoprobe sufficiently below its K_i to prevent RT reversible inhibition. The results given in Table 1 show the time-dependent photoinactivation data for **2**, and Table 2 shows the time-dependent photoinactivation data for **3**. When RT (in the absence of the photoprobe) was photolyzed at 3500 Å, there was consistently no photoinactivation of RT activity observed up to 12 min. Photoinactivation of RT was slightly more efficient for **2** than for **3** as demonstrated by the 21 versus 40% residual RT activity remaining after 6 min photolysis in the presence of 100 μM TCRTI photoprobe, but in both cases the photoinactivation was protected by saturating template/primer but not by dNTP in direct competition experiments.

Table 1. Time-dependent photoinactivation of RT by **2** and substrate protection[a]

Photolysis time (min)[b]	Additions	% Remaining activity[c,d]
0	100 μM **2**	100
6.0	100 μM **2**	21
12.0	100 μM **2**	17
6.0	100 μM **2** + 500 nM poly(rA)·(dT)10	77
6.0	100 μM **2** + 5 mM TTP[e]	28
8.0	None; 3500 Å control	98

[a]Standard reaction conditions: 2 μM RT, 3 mM $MgCl_2$, and 2 mM 2-mercaptoethanol as scavenger with photolysis at 3500 Å.
[b]Photolysis time at 25 °C.
[c]Percent activity remaining after photolysis as measured by initial rate data after dilution of the photolysis mixture.
[d]Errors of at least triplicate determination are within ±5%.
[e]Magnesium concentration was increased to 50 mM to account for the increase in triphosphate.

Table 2. Time-dependent photoinactivation of RT by **3** and substrate protection[a]

Photolysis time (min)[b]	Additions	% Remaining activity[c,d]
0	100 μM **3**	100
1.0	100 μM **3**	60
6.0	100 μM **3**	40
6.0	100 μM **3** + 500 nM poly(rA)·$(dT)_{10}$	95
6.0	None; 3500 Å control	99

[a]Standard reaction conditions: 2 μM RT, 3 mM $MgCl_2$, and 2 mM 2-mercaptoethanol as scavenger with photolysis at 3500 Å.
[b]Photolysis time at 25 °C.
[c]Percent activity remaining after photolysis as measured by initial rate data after dilution of the photolysis mixture.
[d]Errors of at least triplicate determination are within ±5%.

When RT was irradiated at 3500 Å with various concentrations of photoprobes **2** and **3**, there was a concentration-dependent inactivation of enzyme in both cases with saturation at maximum inactivation of about 80 and 60%, respectively (Figs. 3 and 4), data which correlate nicely with the time-dependent photoinactivation data. When fit to an equation assuming that photoinactivation occurs from an enzyme–photoprobe binary complex, the data yielded an EC_{50} of 20 and 25 μM, respectively, which correlates with the average K_i of 10 μM observed in the kinetic inhibition studies.[13] However, a saturating concentration (500 nM) of template/primer essentially blocks the concentration-dependent photoinactivation of RT by **2** at low photoprobe concentration.

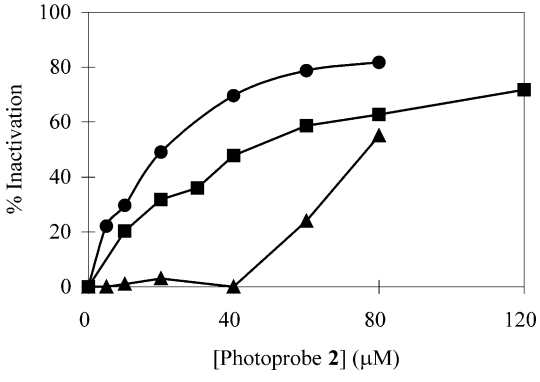

Figure 3. Concentration-dependent photoinactivation of RT by TCRTI photoprobe **2** and substrate protection. The enzyme and photoprobe in the absence (circles) or presence of 500 nM poly (rA)·oligo$(dT)_{10}$ (triangles) or 5 mM TTP (squares). The enzyme, photoprobe and substrate when applicable were incubated in buffer containing mercaptoethanol as scavenger and saturating magnesium chloride (3 mM for control and template-primer experiments and 50 mM for TTP protection), and photolyzed at 3500 Å for 6.0 min. The residual polymerase activity was then determined as described in the Experimental.

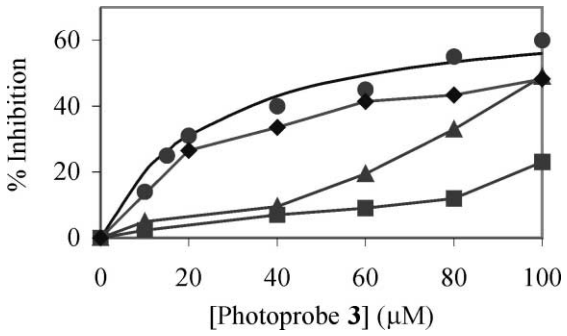

Figure 4. Concentration-dependent photoinactivation of RT by photoprobe **3**. RT was photoinactivated in the presence of only photoprobe **3** (circles), or with both photoprobe **3** and 5 mM TTP (with 50 mM $MgCl_2$) (diamonds), freshly-prepared 60 nM poly (rA)·$(dT)_{10}$ (triangles), or 500 nM freshly-prepared poly(rA)·$(dT)_{10}$ (squares). Each reaction mixture was incubated for 5 min before photolysis at 3500 Å for 6 min, and residual RT activity was assayed as described in the Experimental.

High concentration (i.e., 5 mM) of TTP in 50 mM $MgCl_2$ shifted the dose–response curve for the concentration-dependent inactivation of RT by **2** by a small factor, a protection which was readily overcome at increasing photoprobe concentration. The weak inhibition of RT at even high TTP concentration illustrates the unique binding ability of the TCRTI photoprobes to the free enzyme.

The concentration-dependent photoinactivation of RT by **3** was also protected strongly by template/primer and weakly by TTP. Even at the highest concentration of **3** (i.e., 100 μM), the protection by freshly-prepared, saturating template/primer was still 80%. When the concentration of the template/primer was dropped to 60 nM (i.e., $3\times K_d$ for the template/primer) to establish the pattern of protection by the template/primer, the photoinactivation curve shifts to the right and approaches maximum photoinactivation at higher concentrations of the photoprobe, indicating that at high concentration the TCRTI photoprobe can overcome the protection afforded by template-primer, a result consistent with our conclusion from the kinetic data that the template-primer and TCRTIs compete with the same or overlapping sites on free RT.

As TTP has very weak affinity to the free enzyme form of RT,[21] a high concentration of TTP (5 mM, i.e., $1000\times K_m$ for binary form) was used for photoinactivation protection experiments. As illustrated in Figure 4, in a buffer containing 50 mM $MgCl_2$ (i.e., 10× the concentration of TTP), the dose–response curve has a EC_{50} of 27 μM and maximal photoinactivation of 55%. As both EC_{50} and maximal photoinactivation of the curve in the presence of the high concentration of TTP are very close to those of the curve in the absence of TTP, the exact protective nature of TTP can not be determined unambiguously.

Photoincorporation of TCRTI photoprobes 2 and 3

Photoincorporation experiments using [β,γ-^{32}P]-labeled **2** and **3** were carried out in order to correlate with photoinactivation and to identify the subunits of RT covalently labeled. The 3500 Å photolysis mixtures were denatured with SDS and loaded onto a polyacrylamide gel and subjected to denaturing gel electrophoresis. The resulting gel obtained from photoincorporation of **2** was divided, and one-half was dried and visualized by autoradiography while the second half was stained for protein. The gel obtained for photoincorporation of **3** was first stained for protein with Coomassie blue, dried and scanned by a phosphor imager. The results of photoincorporation and protein staining are shown in Figures 5 and 6 for **2** and **3**, respectively. Photoprobe **2** shows concentration-dependent photoincorporation at 5, 25, and 100 μM, and the photoincorporation is predominantly into the p66 subunit which contains the polymerase active site. At 100 μM the degree of specific photoincorporation into the p66 versus the p51 subunit is >95% based on densitometry scanning of the X-ray film.

Photoprobe **3** is more specific in photolabeling the p66 subunit of RT. The Coomassie blue stain of MW standards and RT, and the phosphor imager scan of photolabeled samples, are shown in Figure 6. Denatured RT shows two bands with molecular weights of approximately 66 and 51 kDa, respectively. For the control experiment, [β,γ-^{32}P]-**3** was pre-irradiated for 15 min and then photolyzed with RT; in this case, there is no radioactivity incorporated into either the 66- or 51-kDa bands of lane 1, suggesting that the photoincorporation

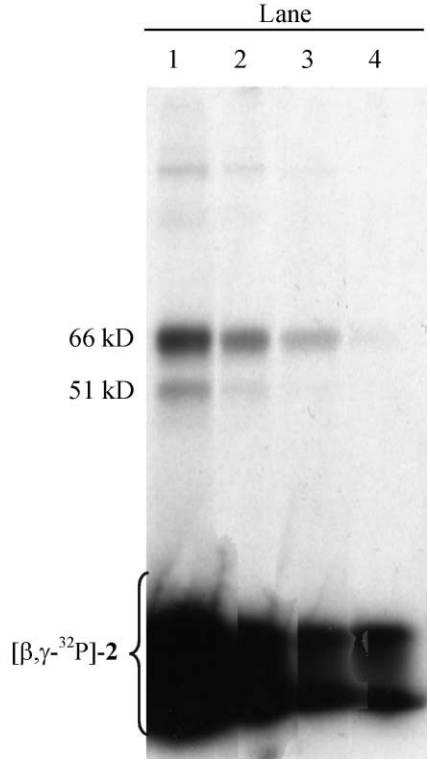

Figure 5. Photoincorporation of [β,γ-^{32}P]-**2** into RT at 3500 Å photolysis for 6 min. RT was photolyzed at 350 nm at photoprobe concentrations of 100, 25, and 5 μM for lanes 1, 2, and 3, respectively. Lane 4 is a control with 5 μM of pre-photolyzed label. The MWs given in the margin were determined from mobility relative to molecular weight standards.

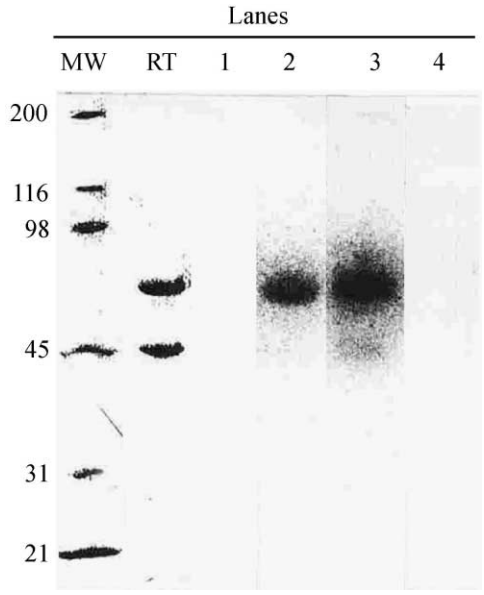

Figure 6. Photoincorporation of [β,γ-^{32}P]-**3** into RT at 3500 Å for 6 min. The Coomassie blue stain lanes are labeled 'MW' for the molecular weight standards (size indicated in kD) and RT for reverse transcriptase. The phosphor-image of the photolyzed samples are shown in lanes 1–4, where: lane 1: RT photolyzed with 40 μM of [β,γ-^{32}P]-**3** pre-irradiated 15 min at 3500 Å light; lane 2: RT photolyzed with 40 μM of [β,γ-^{32}P]-**3**; lane 3: RT photolyzed with 100 μM of [β,γ-^{32}P]-**3**; lane 4: RT was photolyzed with 40 μM of [β,γ-^{32}P]-**3** in the presence of 500 nM poly(rA)·$(dT)_{10}$. In each case the enzyme was pre-incubated with the indicated additions for 5 min, and the solution was photolyzed for 6 min in a water-jacketed quartz cuvette. The samples were then denatured and electrophoresed on SDS-PAGE and treated with both Coomassie stain and phosphor imaging.

of photoprobe **3** into RT is light- and azide dependent. When RT was photolyzed with 40 μM of [β,γ-^{32}P]-**3** (lane 2), incorporation of radioactivity was only observed in the 66-kDa band, which further suggests an active site labeling of the free enzyme. Lane 3 shows the results of RT photoincorporation by 100 μM of [β,γ-^{32}P]-**3**. Densitometry scanning indicates that the ratio of incorporation into the p66 versus the p51 subunits is 100:1. Therefore, the non-specific labeling is small even for the high concentration of photoprobe **3**. In addition, the radioactivity incorporated at the 66-kDa band of lane 3 is approximately twice that at the 66-kDa band of lane 2, a result demonstrating that the covalent incorporation of photoprobe **3** into the p66 subunit is concentration-dependent. Lane 4 shows the result of photoincorporation of **3** into RT in the presence of a saturating concentration of template/primer. The radioactivity of the 66-kD band of lane 4 is barely observed, suggesting that the presence of a saturating concentration of template/primer can compete with the radioactive probe and protect RT from photoincorporation, a result consistent with the time and concentration dependent photoinactivation data.

Binding site identification using photoprobe 2

For identification of the site of covalent incorporation of **2** into RT, the enzyme (1.5 nmol in 750 μL) was photolabeled at 3500 Å with 100 μM photoprobe **2,** and the solution was dialyzed and digested with trypsin at pH 8.0. Instead of using radioactive photoprobe as a tracer for identification of modified peptides, a diode array UV detector was used to identify the photoprobe based on the long wavelength absorbance of its photoproducts above 290 nm. A native tryptic digest of RT was also analyzed and used as a control to further facilitate the identification of the modified fragment(s). The neutral triethylammonium bicarbonate buffer (pH 7.4) was used for peptide mapping on HPLC to minimize non-specific absorption of the nucleotide products to the reverse-phase column.

The HPLC absorbance profiles of the peptide maps of the native and photolabeled RT at 220 (top panel) and 290 nm (bottom panel) are shown in Figure 7. In the top panel, the absorbance profile of photolabeled RT (upper trace) showed three peaks labeled 3, 5, and 6 with retention times of 14.6, 15.6, and 16.1 min, respectively, which were not present in the native enzyme (lower trace). Moreover, these peaks had significant absorbance at 290 nm (bottom panel) which is characteristic of the UV absorbance of the photoproducts of **2** but unlike any absorbance in this region of the native peptide map of RT (upper trace), suggesting that these peaks contain nucleotide photoprobe. Fractions 3, 5, and 6 were then collected separately and repurified by reverse-phase HPLC using a shallow gradient of 0–25% CH3CN in 60 min (Fig. 8). Rechromatography of peak 3 gave two peaks (3-1 and 3-2), both of which have absorbance at 290 nm (Fig. 8); rechromatography of peak 5 gave only one major peak which had absorbance at 290 nm (Fig. 8); and rechromatography of peak 6 showed one major peak (6-3) and 2 minor peaks (6-1, 6-2), but the minor peaks did not have significant absorbance at 290 nm (Fig. 8). The peaks with absorbance at 290 nm from all three fractions were isolated and subjected to N-terminal amino acid sequence analysis.

As shown in Table 3, fragment 3-1 gave no sequence, and the only residue which could be unambiguously assigned for the other peptide sequences was the Gly which was the first residue eluted for peptides 3-2, 5-1, and 6-3. The total Gly released in the first cycle for these three peptides is >137 pmol (two peaks were off scale and only minimum amount could be determined). The short sequence, which we have not observed in other sequencing work, could result from a blocked sequence after Gly. In fact, free glycine is not released in the trypsin digest of RT, and because glycine does not bind to reverse phase under conditions of our chromatography, this residue must be part of a larger sequence. The fragments isolated also have associated uv activity, so the peptide fragments releasing Gly in the first cycle are also likely modified. The only hint as to the sequence in this case is the appearance of Ala in the fourth cycle during the sequence of peptide 6–3. This Ala residue is detected in a small but real quantity. There are only five Gly-? sequences released from RT by trypsin digestion, and the only partial tryptic peptide fragment of RT which matches this Gly-X-X-Ala partial sequence is: Gly^{155}-Ser^{156}-Pro^{157}-Ala^{158}-. Thus, from this data we conclude that Ser^{156} or an adjacent

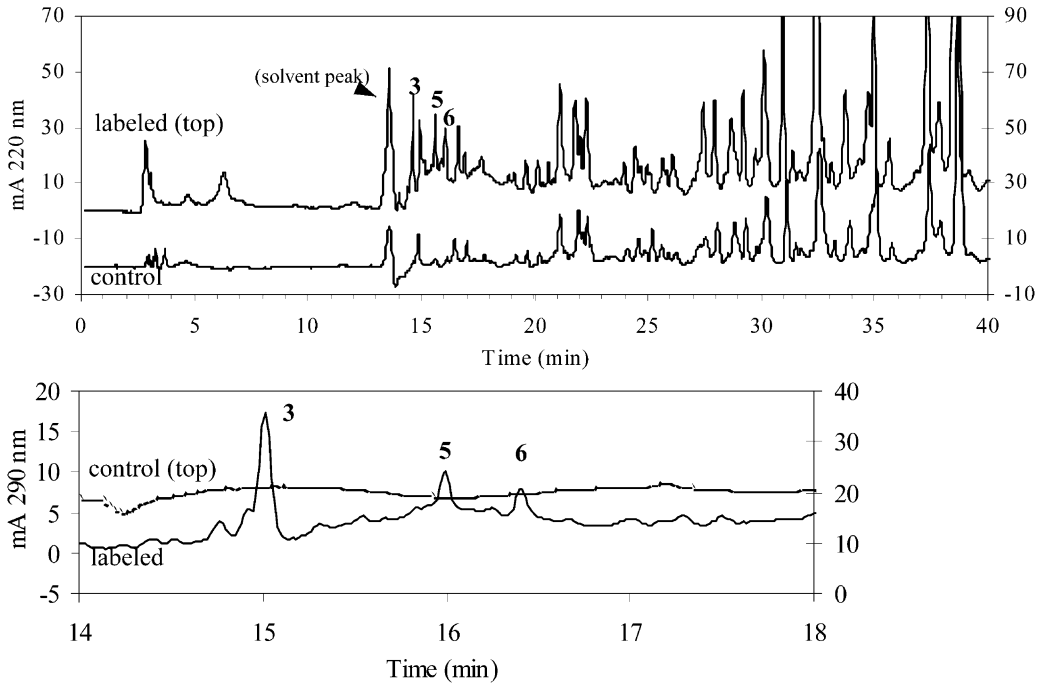

Figure 7. HPLC elution profiles of tryptic digests of reverse transcriptase and reverse transcriptase photolabeled with **2**. Panel A: Absorbance monitored at 220 nm for control (bottom trace) and labeled (top trace) enzyme. Panel B: Absorbance monitored at 290 nm for control (top trace) and labeled (bottom trace) enzyme expanded to cover the time range from 14 to 18 min to show the peaks of interest. Tryptic digests were chromatographed on a C_{18} reverse-phase column eluting with a 60-min gradient of 0–50% acetonitrile in 5 mM triethylammonium bicarbonate buffer.

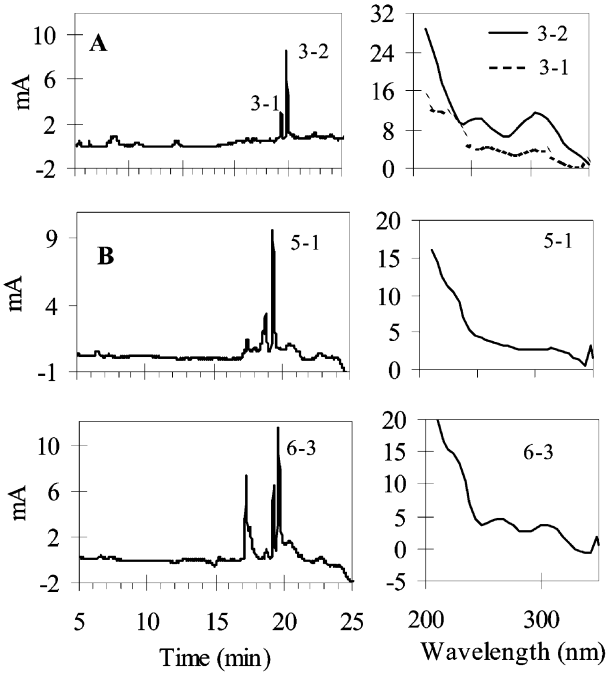

Figure 8. Chromatographic purification of labeled tryptic fragments from RT labeled by **2**. Panel A: Purification of peak 3; Panel B: Purification of peak 5; Panel C: Purification of peak 6. The UV spectra of the peaks labeled in the chromatogram are given in the graph to the right of the HPLC trace. Samples were chromatographed using a 60-min linear gradient of 0–25% acetonitrile in 5 mM triethylammonium bicarbonate.

Table 3. Amino acid sequence analysis of tryptic and V-8 protease fragments of HIV-1RT modified by photoprobe **2** and **3**, respectively

Probe: fraction[a]	Cycle	AA	Yield (pmol)[b]	AA assigned
2: 3-2	1	Gly	>66	—
	2	None		—
	3	None		—
2: 5-1	1	Gly	31	—
2: 6-3	1	Gly	>41	Gly155
	2	None	—	Ser156
	3	None	—	Pro157
	4	Ala	3.03	Ala158
	5	None	—	
3: 1-1	1	X	289	Phe77[c]
	2	R	65	Arg78
	3	E	24	Glu79
3: 2-5	1	K	105	Lys431
	2	E	54	Glu432
	3	P	35	Pro433
	4	K(I)	18	Ile434
	5	V	51	Val435
	6	G	51	Gly436
	7	A	31	Ala437
	8	E	7	Glu438

[a]Fraction 3–1, from probe **2**, and fractions 2-1, 2-2, 2-3, and 2-4 from probe **3** showed no sequence data.
[b]Yield of the PTH derivative based on peak area relative to that of a 30 pmol standard.
[c]The Phe residue was assigned based on subsequent sequence data.

residue is the amino acid residue that is covalently modified by photoprobe **2**. The blocked sequence is most likely to arise from the β-OH modification of serine, as *O*-acyl and *O*-alkyl modifications on serine are known to block sequence progression.[22] Based on the total amount of Gly residue released in the sequencing, we estimate a total yield from photolabeling, dialysis, trypsin cleavage, two HPLC purifications and sequencing of 76% yield at each step.

Binding site identification using photoprobe 3

In order to identify the site labeled by **3**, RT (5000 pmol) was photolabeled with 100 μM [β,γ-^{32}P]-**3**, and the photolysis mixture was dialyzed against 50 mM ammonium bicarbonate buffer, pH 7.1, to remove unbound photoprobe **3**. Control experiments showed that the photolabel triphosphate is stable to these conditions. The resulting solution contained 2637 pmol (53% incorporation) of irreversibly bound radioactivity and was lyophilized to dryness. The residue was suspended in 50 mM potassium phosphate and centrifuged, resulting in an insoluble pellet containing 581 pmol (22%) and a supernatant containing 2056 pmol (78%) of radioactivity; the supernatant was subsequently digested with V-8 protease (1:30 protease to RT ratio). The resulting peptide fragments were separated by reverse phase HPLC yielding two radioactive peaks with retention times 4–8 and 18–21 min, respectively, with radioactivity recovery of 72% of applied sample (Fig. 9, panel A). The shorter retention time peak contained 651 pmol (32%) of bound radioactivity, while the other peak contained 456 pmol (22%) of bound radioactivity.

Rechromatography of the peak with retention time 4–8 min resulted in the isolation of a major peak containing 360 pmol (55%) of irreversibly bound radioactivity (Fig. 9, panel B). The radioactivity recovery rate was 87% of applied sample. The fractions corresponding to the major peak (retention time 4–5 min) were collected and lyophilized. The residue was sequenced using N-terminal Edman degradation method. The amino acid sequence of the fragment was XRE, where X does not correspond to a natural amino acid (Table 3). N-Terminal sequencing indicates that the yield for residues X, R, E is 289, 64, and 28 pmol, respectively. The sequence of the radioactive fragment was compared to the V-8 protease digest map of RT. The only polymerase V8 protease fragment with the sequence XRE is the sequence ^{77}FRE located in the β4 strand of the fingers subdomain.

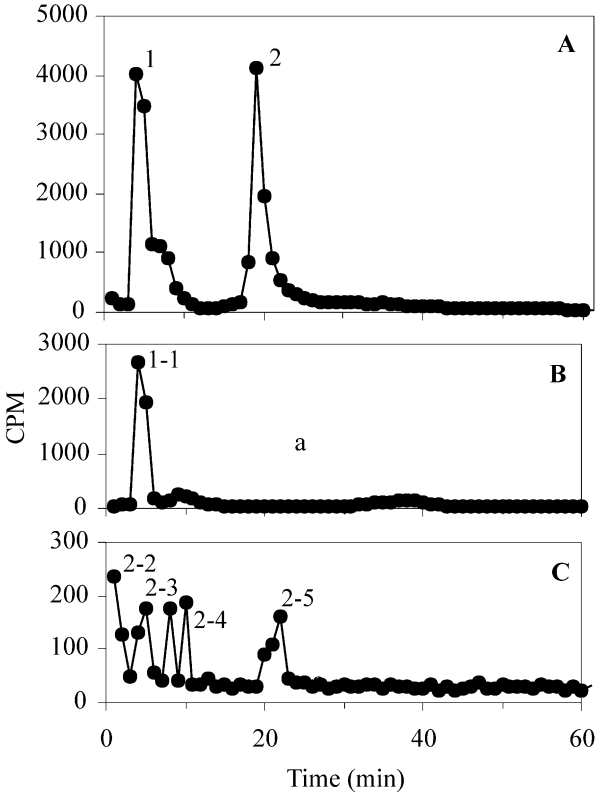

Figure 9. HPLC separation of V-8 protease digestion fragments from ^{32}P-**3** labeled RT: (A) plot of radioactivity as a function of retention time for the crude sample; (B) rechromatography of the radioactive peak with retention time 4–8 min in panel A; (C) rechromatography of the radioactive peak with retention time 18–21 min in panel A.

Rechromatography of the peak with retention time 18–21 min gave several radioactive peaks with a total radioactivity recovery of 47% (Fig. 9, panel C). The peaks at 1–2, 4–5, 8–10, 20–22 min contained 46, 39, 51, and 45 pmol of irreversibly bound radioactivity, respectively. With the exception of the 20–22 min peak, none of the other isolated radioactive peaks showed a sequence. Edman analysis indicated that the peak with retention time 20–22 min contained the amino acid sequence ^{431}KEPIVGAE, which is located in a connecting strand between the connection and ribonuclease H domains. The sequence showed no discernable site of modification by the radiolabeled nucleotide, and the release of amino acids (100 pmol in first turn) is >twice that predicted by the radioactivity content, suggesting that the peptide and photoprobe may have co-eluted.

Discussion

Our initial approach to photoprobes of DNA polymerases and RTs was based on a thermodynamic model proposed by Doronin and Kolocheva for binding of substrates to this class of enzymes.[23,24] The triphosphates of dNTP's contribute about −5.9 to −6.7 kcal/mol binding energy, while the remaining binding interactions are due to complementary base pairing to template and base stacking with primer. In order for dNTP's to bind enzyme in the absence of template/primer substrate, we appended minor groove substituents to the 2-position of dATP in order to provide anchoring interactions to a lipophilic pocket in the template domain (as proposed by Doronin and Kolocheva, see above). The most successful of these photoprobes is 2′-deoxynucleotide **6**, which with a three atom tether between the adenosine and azidophenyl ring is the most active, with a low micromolar inhibition constant for DNA polymerase I Klenow Fragment.[14] We were able to demonstrate that as designed the phenacyl side chain makes contact with a lipophilic domain at the juncture of helices M, N, and O in the template-binding fingers domain of this enzyme.[15] Unfortunately, these inhibitors were not active against reverse transcriptase up to mM concentrations.

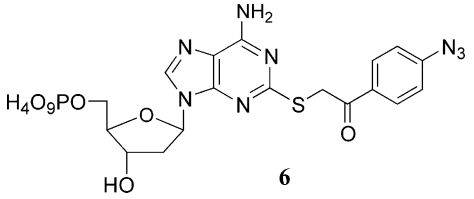

6

The etheno series was then produced with the expectation that increased lipophilicity might increase activity of this class of nucleotide inhibitors. Although derivatives such as **2** are less active than **6** as inhibitors of DNA polymerase Klenow fragment, they show surprising inhibitory activity versus HIV-1 reverse transcriptase. The kinetic data indicate competitive inhibition relative to template-primer and non-competitive relative to dNTPs, suggesting that this class of RT inhibitors bind only to the free form of enzyme and not to the binary enzyme-template/primer as a dNTP substrate.[13] The data supported our design criteria and suggest the TCRTIs differ significantly in binding interaction relative to both the activated NRTIs and the NNRTIs.

To further characterize the binding site for this class of RT inhibitors, the TCRTI photoprobes **2** and **3** were analyzed for their ability to photoinactivate and incorporate into RT. In experiments in which only photoprobe **2** or **3** are incubated alone with RT, photolysis results in both time- and concentration-dependent photoinactivation. The time-dependent photoinactivation correlates with the time-dependent decomposition of both **2** and **3**. Because the photodecomposition products resulting from **2** have an intact etheno group but a decomposed azido, the photoinactivation of RT then correlates specifically to azido decomposition (at lower wavelengths of light the etheno group is photoactive). The time-dependent inactivation of RT by both **2** and **3** is protected nearly completely in simple competitive experiments in which template-primer is added to the mixture of enzyme and photoprobe. Similar protection by dNTP substrates was small or non-existent at mM concentrations of protectant, substantiating earlier evidence that the dNTPs have little affinity for free enzyme (i.e., in the absence of template-primer).

The concentration-dependent photoinactivation data displayed saturation behavior for both photoprobes **2** and **3**, with similar EC_{50}'s (about 20 μM), but with higher maximum inactivation for TCRTI probe **2**. The EC_{50} was calculated based on an equation which requires equilibrium formation of a binary enzyme–photoprobe complex, where photoactivation of the azide and enzyme inactivation occur from this complex; the model does not include inhibition by photo-products or release of activated nitrene. Thus at best the EC_{50} is an approximate $K_{D,app}$, which correlates within a factor of 2 with the average K_i determined from kinetic analyses.[13] The presence of low to saturating concentrations of template-primer shifted the dose–response curve for inactivation of RT by both **2** and **3**, and this substrate protection was overcome by high photoprobe concentration. This behavior, a shift of a dose–response curve to the right without significant change in the maximum effect, is classic evidence for a competitive protection by template/primer. TTP, the complementary dNTP used in the kinetic analysis, was weakly effective at 5 mM concentration as long as the magnesium concentration was kept high. In the case of **2** and **3**, the dose–response curve was shifted by no more than 2-fold, indicating again the weak binding of TTP to the free enzyme and the weak protective nature of dNTPs.

The most compelling evidence for the binding of probes **2** and **3** to the free enzyme is in the photoincorporation experiments for [β,γ-^{32}P]-**2** and [β,γ-^{32}P]-**3**. Both radiolabeled photoprobes displayed concentration-dependent photoincorporation into the p66 subunit of RT. The photoincorporation required an intact azido, and was readily protected by template/primer. Thus the photoincorporation data correlates well with both the time- and concentration-dependent photoinactivation data. Only for probe **2** was there a significant amount of non-specific labeling to the p51 subunit, indicating a high degree of binding specificity for that subunit which contains the polymerase active site.

Determination of the site of modification was more problematic than either the convincing photoinactivation or photoincorporation data. Particularly, with photoprobe **2** the sequence data obtained from the tryptic peptides obtained by HPLC separation and diode-array detection gave incomplete sequence results. The sequencing yield dropped dramatically after a Gly and preceding a presumed Ser residue, so the site of modification could only tentatively be assigned to Ser^{156} (Fig. 10). Because the sequencing problems likely resulted from the demonstrated rearrangement chemistry of the phenylazide, we designed photoprobe **3** in order to overcome the electrophilic behavior of rearranged nitrenes.[19] The V8-protease peptide fragments isolated from the photoincorporation of [β,γ-^{32}P]-**3** were isolated by following the elution of ^{32}P from a C-18 reverse-phase column. Of the five fragments isolated on repurification, only two showed a peptide sequence, and of those only fragment 1-1 with the highest specific activity clearly showed a site of modification. The first residue eluted between Pro and His/Val, but the remaining sequence identified the modified residue as Phe^{77}, which is located on the carboxyl-terminal of β4 of the fingers subdomain at the juncture between the fingers and palm subdomains (Fig. 10). However, this identification cannot be considered definitive since a second peptide eluting at later retention times gave a sequence for a read-through V8 fragment located on the surface in the connection domain and well outside the polymerase site. Thus a definitive site of modification of **3** cannot be assigned.

Our original design of the TCRTIs required significant interactions between two binding sites: the dNTP portion was designed to bind to the triphosphate binding site through magnesium chelation, and the 2-position side chain was designed to interact with potential lipophilic sites in the template binding domain (Fig. 11). The residues tentatively identified as part of the side-chain binding site in the polymerase active site, namely, Ser^{156} and Phe^{77}, are both located in a region called the 'template grip'. This region, which includes β4, αB, β8-αE connecting loop, and β5a structural elements, has significant contacts with the template as revealed by the co-crystal structure of RT bound to double stranded DNA.[2,6] Clearly, our inability to definitively locate the binding site for the TCRTIs does not negate the results

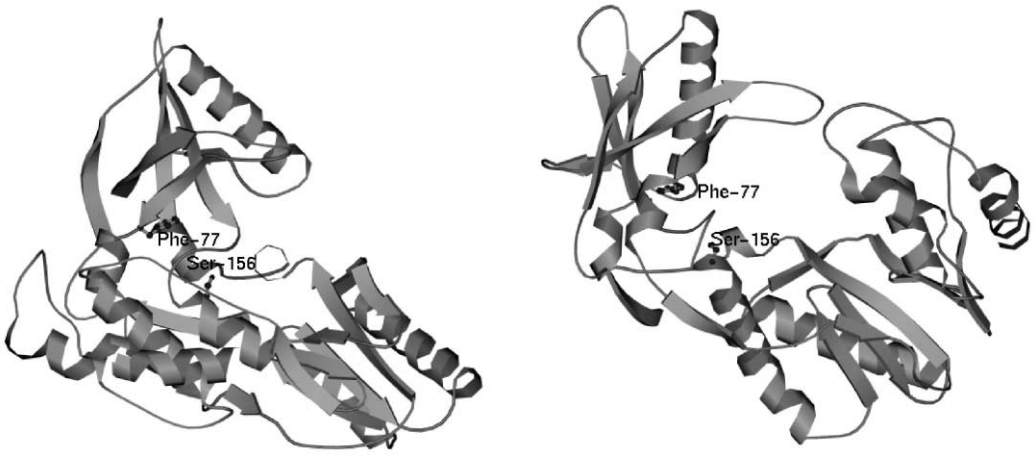

Figure 10. Monoviews of HIV-1 RT polymerase domain labeling sites proposed for TCRTI photoprobes **2** and **3**. The two views are rotated by 90°. The view on the left looks down on the palm, and the view on the right shows the DNA binding cleft.

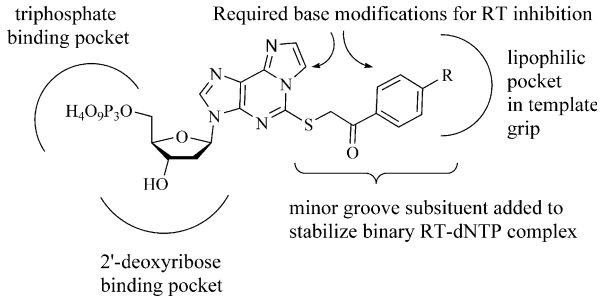

Figure 11. Binding model proposed for the interaction of TCRTIs with HIV-1 RT. The model illustrates the bisubstrate nature of the interaction, with the dNTP portion binding the triphosphate site and the 2-position side chain binding to a template site.

of the kinetic, photoinactivation, photoincorporation, and protection data which suggest the TCRTIs are bisubstrate, or combined substrate, inhibitors as designed, and as such represent a unique target for the inhibition of HIV-1 RT.

Experimental

Materials and equipment

The monophosphate and triphosphate derivatives of photoprobes **2** and **3** were synthesized from 2-thio-1,N^6-etheno-2′-deoxyadenosine 5′-monphopshate as previously described.[13] The [β,γ-^{32}P] derivatives of **2** and **3** were synthesized as described for the synthesis of **2** and **3** with the exception that tributylammonium pyrophosphate was doped with tetrasodium [^{32}P]-pyrophosphate to a specific activity of 200 cpm/pmol and dried prior to use. HIV-1 RT and V-8 protease were purchased from Worthington Biochemical Corporation (Freehold, NJ, USA). Thymidine triphosphate, poly(rA) $(dT)_{10}$ (for studies with 2) and poly(rA) and oligo$(dT)_{10}$ components for freshly-prepared poly(rA) $(dT)_{10}$ (for studies with **3**) were purchased from Pharmacia (Piscataway, NJ, USA). Tritiated thymidine triphosphate was purchased from DuPont New England Nuclear (Boston, MA, USA). Bovine serum albumin was purchased from Sigma (St. Louis, MO, USA). BCA protein assay reagents and Slide-A-Lyzer cassettes (molecular weight cut off 10,000) were purchased from Pierce (Rockford, IL, USA). Whatman DE 81 diethylaminoethyl cellulose paper and Scintiverse II were purchased from Fisher Scientific (Pittsburgh, PA, USA).

Photolysis was conducted in a Rayonet Photochemical Mini-Reactor chamber Model RMR-600 purchased from the Southern New England Ultraviolet Company (Branford, CT, USA). Samples were photolyzed in 1- or 2-mL water jacketed quartz cells. Liquid scintillation counting was conducted in a Packard 1900 TR liquid scintillation counter (Meridian, CT, USA). SDS gel electrophoresis was performed on a Protean II unit and gels were dried on a Model 543 gel drier from BioRad (Richmond, CA, USA). The dried gel was exposed either to a Kodak phosphor image screen (20×25 cm) from Bio-RAD (Richmond, CA, USA) and scanned by a molecular imager FX using software Quantity One from Bio-RAD (Richmond, CA, USA) or to an X-ray film. Reverse phase high pressure liquid chromatography (HPLC) was performed on a Beckman dual pump gradient HPLC system with System Gold software on a Vydac C-4 or C-18 analytical column. Amino acid sequence analysis was contracted to Kansas State University Biotech Core Facility.

Photochemistry of 2 and 3

The monophosphates of nucleotides **2** and **3** (approximately 0.5 mM) were irradiated at 3000 and 3500 Å at room temperature in a quartz cuvette. At indicated time points, aliquots of 30 μL were taken and diluted in 0.1 N HCl (1 mL). The UV spectra of the diluted samples were recorded; the absorbances at 2930 and 3150 Å for **2** and **3**, respectively, were plotted as a function of time, and half-lives for photodecomposition were determined by fitting the data to the equation:

$$\mathrm{Ln}[(A_t - A_\infty)/(A_0 - A_\infty)] = -kt \quad (1)$$

where A_∞ is the absorbance at infinite time of photolysis, A_t is the absorbance at time t, A_0 is the initial absorbance, and k is the first-order rate constant for the photodecomposition.

Structural determination of the photoproducts of 2-(4-azidophenacyl)thio-1,N^6-etheno-dAMP (2m). Compound **2m** (10 mg, 1.1×10^{-3} M) was dissolved in water (15 mL) and irradiated at 3000 Å in a quartz cuvette for 2 min. The reaction mixture was lyophilized to dryness, and the resulting solid was dissolved in H_2O (500 μL) and subjected to HPLC purification on an analytical C18 column eluting with a 30 min linear gradient from 0 to 50% CH_3CN in neutral 10 mM ammonium acetate. Appropriate fractions were pooled and lyophilized, and the structures of the purified products were determined by MS and proton NMR.

Ammonium 2-(S-[3H-diazepinon-4-yl]thio)-1,N^6-etheno-dAMP (4). NMR (D_2O) δ 2.38 (m, 1H, C2′H1), 2.71 (m, 1H, C2′H2), 3.14 (d, $J=6.6$ Hz, 2H, methylenyl H in azepinone), 3.90 (m, 2H, C5′H), 4.11(br s, 1H, C4′H), 4.55 (br s, 1H, C3′H), 6.21 (t, $J=6.9$ Hz, 1H, C1′H), 6.35 (d, $J=10.8$ Hz, 1H, C5″H), 6.46 (dd, $J_1=6.6$ Hz, $J_2=10.8$ Hz, 1H, C6″H), 7.00 (t, $J=6.6$ Hz, 1H, C7″H), 7.86 (s, 1H, C10H), 8.05 (s, 1H, C11H), 8.52 (s, 1H, C8H); high resolution MS (-FAB, glycerol) *m/e* 535.0802; calcd for $C_{20}H_{21}N_6O_8P_1S_1$ ($M-H^+$), 535.0801.

Ammonium 2-(4-aminophenacyl)thio-1,N^6-etheno-dAMP (5). NMR (D_2O) δ 2.00 (m, 1H, C2′H1), 2.55 (m, 1H, C2′H2), 3.82, (m, 2H, C5′H), 3.90 (d, $J_2=10.3$ Hz, 2H, α-methylenyl H), 4.17 (m, 1H, C4′H), 4.54 (m, 1H, C3′H), 5.87 (t, $J=6.9$ Hz, 1H, C1′H), 6.78 (d, $J=8.7$ Hz, 2H, PhH), 7.84 (d, $J=2.4$ Hz, 1H, C10H), 7.93 (d, $J=8.7$ Hz, 2H, PhH), 8.06 (d, $J=2.4$ Hz, 1H, C11H), 8.44 (s, 1H, C8H); high-resolution MS (-FAB, glycerol) *m/e* 519.0867; calcd for $C_{20}H_{21}N_6O_7P_1S_1$ ($M-H^+$), 519.0852.

General RT assay protocol

RT was dialyzed against 50 mM ammonium bicarbonate buffer, pH 7.1, containing 2 mM β-mercaptoethanol and 15% glycerol using Slide-A-Lyzer cassettes at 4 °C over 8 h to remove DTT. Polymerase activity assays were performed in 50 mM Tris–HCl buffer (pH 7.4) containing 3 mM $MgCl_2$, 1 mg/mL of BSA, 60 nM template/primer, and 60 μM ^{3}H-TTP, and the reaction was initiated by addition of the enzyme solution (final concentration of 0.04 units) to the substrate solution to 80 μL total volume. The reaction was incubated at 37 °C for 30 min and quenched by addition of 80 μL of 30 mM EDTA. Aliquots of 20 μL were then spotted on DEAE cellulose paper in triplicate, and the papers were washed in ammonium formate solution (0.3 M, pH 8, 3×200 mL) with gentle stirring, dehydrated in ethanol (200 mL) and ethyl ether (200 mL) and air-dried. The radioactivity on each paper was measured by scintillation counting in 5 mL of Scintiverse II. The initial rate of polymerization was determined as the picomoles of ^{3}HTTP incorporated into DNA per min.

Photoinactivation of RT by photoprobes 2 and 3

A standard photolysis mixture contained 2 μM RT, 2 mM β-mercaptoethanol, 3 mM $MgCl_2$, and 100 μM (time-dependent photoinactivation) or 10–100 μM (concentration-dependent photoinactivation) of the photoprobe in the presence or absence of 60 or 500 nM poly(rA)$(dT)_{10}$ or 5 mM TTP (with 50 mM $MgCl_2$) in assay buffer in a total volume of 80 μL. The photolysis mixture was pre-incubated at 37 °C for 5 min in the dark and subsequently irradiated at 3500 Å at room temperature. Aliquots of 4 μL were removed at indicated times and diluted 25-fold in assay buffer, and an aliquot of 20 μL of the diluted sample was assayed for residual polymerase activity in a total volume of 80 μL. The photoinactivation percentage was calculated as the percentage loss of enzyme activity relative to the enzyme activity of the control assay determined at time 0 before photolysis. The percentage of photoinactivation and photoprobe concentrations were fit into the equation:

$$P_I = \frac{[I]\cdot P_{max}}{[I] + EC_{50}} \quad (2)$$

where P_I is the percent of photoinactivation in the presence of a given probe concentration, P_{max} is the maximum inactivation at saturation, I is the photoprobe concentration and EC_{50} is the concentration of the photoprobe resulting in 50% of maximum photoinactivation of the enzyme. Parameters P_{max} and EC_{50} was calculated by nonlinear regression analysis using the program MINSQ.

Photoincorporation of [β,γ-^{32}P]-2 and [β,γ-^{32}P]-3 into RT

RT (2.5 μM) was mixed with various concentrations of [β,γ-^{32}P]-**2** or [β,γ-^{32}P]-**3**, 2 mM β-mercaptoethanol, 3 mM $MgCl_2$ in the presence or absence of 500 nM template/primer in 50 mM Tris–HCl buffer (pH 7.4) in a total volume of 40 μL. The mixture was incubated at 37 °C for 5 min in the dark and subsequently irradiated at 350 nm for 6 min at room temperature. For the control experiment, 20 μM of ^{32}P-labeled photoprobe **3** was pre-irradiated for 15 min before addition to the enzyme solution. The photolysis mixtures were diluted with 2-times treatment buffer (50 mM Tris–HCl, pH 6.8, containing 100 mM dithiothreitol, 2% SDS, 10% glycerol, and 1% bromophenol blue) and denatured by heating on a boiling water bath for 3 min. The denatured samples were loaded on a polyacrylamide gel in which stacking and resolving gels were composed of 4 and 12% acrylamide monomer, respectively, and electrophoresis was carried out at 12 mA for 7 h. For **2**, the duplicate gel was divided, and one half was stained with Coomassie Blue prior to drying. For autoradiography, the gel was fixed in destaining solution (10% acetic acid, 5% methanol, and 85% water), and the dried gel was exposed to Kodak XRA-5 X-ray film in a cassette with intensifying screen. After 5 days at −70 °C, the film was developed, and band intensities were measured by densitometry scanning.

For **3**, the gel was subjected to Coomassie blue stain and dried at 80 °C for 1.5 h. The dried gel was exposed to a Kodak phosphor image screen (20×25 cm, Bio-Rad) for 24 h and subsequently scanned by a molecular imager FX (Bio-Rad). The data were processed using the software Quantity One (Bio-Rad).

Peptide mapping for TCRTI probe 2

A photolysis mixture containing RT (2 μM) in the absence (control) or presence of photoprobe **2** (100 μM) in a total volume of 750 μL or 50 mM Tris–HCl buffer, pH 7.4 containing 3 mM $MgCl_2$ and 2 mM 2-mercaptoethanol was incubated at 37 °C for 10 min and irradiated at 3500 Å for 15 min. The mixture was dialyzed (MWCO: 2000) against 50 mM ammonium bicarbonate buffer (pH 8.0, 4×500 mL) at 10 °C to remove the unbound photoprobe and lyophilized to dryness. The resulting solid was then dissolved in 1.25 mL of ammonium bicarbonate buffer (50 mM, pH 8.0) to which freshly-prepared trypsin solution (1/50 molar equivalent) was added. After 2 h incubation at 37 °C, an equivalent amount of freshly-prepared trypsin solution was added and incubated overnight at 37 °C. The tryptic digests were analyzed by reverse-phase HPLC using a 60-min linear gradient of acetonitrile from 0 to 50% in triethylammonium bicarbonate buffer (TEABC, 5 mM, pH 7.4). Peptides maps were monitored simultaneously at 220 and 290 nm. Fractions that had significant absorbance at 290 nm and were not present in the tryptic map of the native RT were collected, pooled and repurified by HPLC using a shallower elution gradient (a 60-min linear gradient of 0–25% acetonitrile in TEABC buffer). Fractions of interest were pooled and dried on a speed-vac, and the amino-acid sequence analysis of these fractions were performed by Edman degradation.

Peptide mapping for [β,γ-^{32}P]-3

A mixture containing 2.5 μM RT, 100 μM [β,γ-^{32}P]-**3**, 2 mM β-mercaptoethanol, 3 mM $MgCl_2$ in 50 mM Tris–HCl buffer (pH 7.4) in a total volume of 2000 μL was incubated at 10 min in the dark and photolyzed at 350 nm for 15 min. The photolysis mixture was transferred to a Slide-A-Lyzer cassette (molecular weight cutoff 10,000) and dialyzed against 4×500 mL of 50 mM ammonium bicarbonate buffer, pH 7.1 containing 2 mM β-mercaptoethanol and 15% glycerol at 4 °C over 27 h. The dialyzed enzyme solution was lyophilized to dryness, and the resulting residue was suspended in 50 mM potassium phosphate. The supernatant (containing 78% of the radioactivity) was separated by centrifugation, mixed with 19.5 μg of V-8 protease (a 1:30 protease to RT ratio), and the solution was incubated at 37 C for 18 h. The peptides after protease digestion were separated by HPLC on a Vydac C_{18} analytical column using a gradient elution from 5 mM triethylammonium bicarbonate in water (buffer A, pH 7.4) to 5 mM triethylammonium bicarbonate in 50% acetonitrile (buffer B, pH 7.4) over 60 min at a flow rate 1.0 mL/min. Fractions were collected at 2-min intervals and counted for radioactivity without cocktail. Fractions comprising the single peak of radioactivity were recovered and pooled, lyophilized in a siliconized polyethylene tube, and subjected to HPLC with a gradient from 100% Buffer A to 50% Buffer B over 60 min. All peaks containing radioactivity were collected and lyophilized to dryness. The resulting samples were sequenced using the N-terminal Edman degradation method.

References and Notes

1. Chandra, A.; Gerber, T.; Kaul, S.; Wolf, C.; Demirhan, I.; Chandra, P. *FEBS Lett*. **1986**, *200*, 327.
2. Jacobo-Molina, A.; Ding, J.; Nanni, R. G.; Clark, A. D.; Lu, X.; Tantillo, C.; Williams, R. L.; Kamer, G.; Ferris, A. L.; Clark, P.; Hizi, A.; Hughes, S. H.; Arnold, E. *Proc. Natl. Acad. Sci. U.S.A*. **1993**, *90*, 6320.
3. Kohlstaedt, L. A.; Wang, J.; Friedman, J. M.; Rice, P. A.; Steitz, T. A. *Science* **1992**, *256*, 1783.
4. Di Marzo Veronese, F.; Copeland, T. D.; DeVico, A. L.; Rahman, R.; Oroszlan, S.; Gallo, R. C.; Sarngadharan, M. G. *Science* **1986**, *231*, 1289.
5. Pop, M.; Biebricher, C. *Biochemistry* **1996**, *35*, 5054.
6. Huang, H.; Chopra, R.; Verdine, G. L.; Harrison, S. C. *Science* **1998**, *282*, 1669.
7. Wu, J. C.; Warren, T. C.; Adams, J.; Proudfoot, J.; Skiles, J.; Raghavan, P.; Perry, C.; Potocki, I.; Farina, P. R.; Grob, P. M. *Biochemistry* **1991**, *30*, 2022.
8. Cohen, K. A.; Hopkins, J.; Ingraham, R. H.; Pargellis, C.; Wu, J. C.; Palladino, D. E. H.; Kinkade, P.; Warren, T. C.; Rogers, S.; Adams, J.; Farina, P. R.; Grob, P. M. *J. Biol. Chem*. **1991**, *266*, 14670.
9. Pauwels, R.; Andries, K.; Debyser, Z.; Van Daele, P.; Schols, D.; Stoffels, P.; Vreese, K. D.; Woestenborghs, R.; Vandamme, A.-M.; Janssen, C. G. M.; Cauwenbergh, G.; Desmyter, J.; Heykants, J.; Janssen, M. A. C.; Clercq, E. D.; Janssen, P. A. J. *Proc. Natl. Acad. Sci. U.S.A*. **1993**, *90*, 1711.
10. Ding, J.; Das, K.; Tantillo, C.; Zhang, A.; Clark, A. D.; Jessen, S.; Lu, X.; Hsiou, Y.; Jacobo-Molina, A.; Andries, K.; Pauwels, R.; Moereels, H.; Koymans, L.; Janssen, P. A. J.; Smith, R. H., Jr.; Kroeger Koepke, M.; Michejda, C. J.; Hughes, S. J.; Hughes, S. H.; Arnold, E. *Structure* **1995**, *3*, 365.
11. Ding, J.; Das, K.; Moereels, H.; Koymans, L.; Andries, K.; Janssen, P. A. J.; Hughes, S. H.; Arnold, E. *Struct. Biol*. **1995**, *2*, 407.
12. De Clercq, E. *Il Farmaco* **1999**, *54*, 26.
13. Li, K.; Lin, W.; Chong, K. H.; Moore, B. M.; Doughty, M. B. *Bioorg. Med. Chem*. **2002**, *10*, 507.
14. Moore, B. M.; Li, K.; Doughty, M. B. *Biochemistry* **1996**, *35*, 11634.
15. Moore, B. M.; Jalluri, R.; Doughty, M. B. *Biochemistry* **1996**, *36*, 11642.
16. Mair, A. C.; Stevens, E. F. V. *J. Chem. Soc. C* **1971**, 2317.
17. Nielsen, P. E.; Buchardt, O. *Photochem. Photobiol*. **1982**, *35*, 317.
18. Purvis, R.; Smalley, R. K.; Strachan, W. A.; Suschitzky, H. *J. Chem. Soc., Perkin Trans. 1* **1978**, 191.
19. Poe, R.; Schnapp, K.; Young, M.; Grayzar, J.; Platz, M. *J. Am. Chem. Soc*. **1992**, 5054.
20. Crocker, P. J.; Imai, N.; Rajagopalan, K.; Boggess, M. A.; Kwiatkowski, S.; Dwyer, L. D.; Vanaman, T. C.; Watt, D. S. *Bioconjugate Chem*. **1990**, *1*, 419.
21. Delahunty, M. D.; Wilson, S. H.; Karpel, R. L. *J. Mol. Biol*. **1994**, *236*, 469.
22. Geisow, M. J., Aitken, A. In *Protein Sequencing: A Practical Approach*; Findlay, J., Geisow, M., Eds.; IRL: New York, 1989; p 85.
23. Doronin, S. V.; Lavrik, O. I.; Nevinsky, G. A.; Podust, V. N. *FEBS Lett*. **1987**, *216*, 221.
24. Kolocheva, T. I.; Nevinsky, G. A.; Levina, A. S.; Khomov, V. V.; Lavrik, O. I. *J. Biomol. Struc. Dynam*. **1991**, *9*, 169.